

# A Gain-of-function Mutation in Adenylate Cyclase Confers Isoflurane Resistance in *Caenorhabditis elegans*

Owais Saifee, M.D., Ph.D.,\* Laura B. Metz, B.Sc.,† Michael L. Nonet, Ph.D.,‡  
C. Michael Crowder, M.D., Ph.D.§

## ABSTRACT

**Background:** Volatile general anesthetics inhibit neurotransmitter release by a mechanism not fully understood. Genetic evidence in *Caenorhabditis elegans* has shown that a major mechanism of action of volatile anesthetics acting at clinical concentrations in this animal is presynaptic inhibition of neurotransmission. To define additional components of this presynaptic volatile anesthetic mechanism, *C. elegans* mutants isolated as phenotypic suppressors of a mutation in syntaxin, an essential component of the neurotransmitter release machinery, were screened for anesthetic sensitivity phenotypes.

**Methods:** Sensitivity to isoflurane concentrations was measured in locomotion assays on adult *C. elegans*. Sensitivity to the acetylcholinesterase inhibitor aldicarb was used as an assay for the global level of *C. elegans* acetylcholine release. Comparisons of isoflurane sensitivity (measured by the EC<sub>50</sub>) were made by simultaneous curve-fitting and F test.

**Results:** Among the syntaxin suppressor mutants, *js127* was the most isoflurane resistant, with an EC<sub>50</sub> more than 3-fold that of wild type. Genetic mapping, sequencing, and transformation phenocopy showed that *js127* was an allele of *acy-1*, which encodes an adenylate cyclase expressed throughout the *C. elegans* nervous system and in muscle. *js127* behaved as a gain-of-function mutation in *acy-1* and had in-

## What We Already Know about This Topic

- Although volatile general anesthetics inhibit neurotransmitter release by a mechanism not fully understood, genetic evidence in *Caenorhabditis elegans* has shown that a major mechanism of action of volatile anesthetics acting at clinical concentrations in this animal is presynaptic inhibition of neurotransmission

## What This Article Tells Us That Is New

- An additional component of the presynaptic volatile anesthetic mechanism was demonstrated by showing that activation of neuronal adenylate cyclase antagonizes isoflurane inhibition of locomotion in *C. elegans*

creased concentrations of cyclic adenosine monophosphate. Testing of single and double mutants along with selective tissue expression of the *js127* mutation revealed that *acy-1* acts in neurons within a G $\alpha_s$ -PKA-UNC-13–dependent pathway to regulate behavior and isoflurane sensitivity.

**Conclusions:** Activation of neuronal adenylate cyclase antagonizes isoflurane inhibition of locomotion in *C. elegans*.

VOLATILE general anesthetics (VAs) have a complex set of actions on neurotransmission that summate to produce general anesthesia.<sup>1</sup> VAs promote inhibitory synaptic transmission by potentiation of  $\gamma$ -aminobutyric acid type A and glycine receptors and decrease excitatory transmission by multiple potential mechanisms. Transmitter release is reduced at both inhibitory and excitatory synapses by VAs, but VA potency and efficacy are greater at excitatory synapses.<sup>1</sup> Thus, the net presynaptic VA effect should be a decrease in central nervous system excitability. Biochemical and electrophysiologic evidence have implicated inhibition of sodium channels as one molecular mechanism whereby VAs inhibit neurotransmitter release.<sup>1</sup> However, blockade of sodium channels does not account for the entire inhibition of transmitter release, at least at some synapses<sup>2</sup>; rather, the transmitter release machinery that lies mechanistically downstream of the sodium channel is a good candidate as the residual VA target.

In the nematode *Caenorhabditis elegans*, we found that an unusual mutation in the *unc-64* gene, which encodes *C. elegans* neuronal syntaxin, fully blocked the behavioral effects of clinical concentrations of isoflurane (by this we mean concentrations that fall within the range used for human anesthesia, as much as two times the minimum alveolar concen-

\* Graduate Student, ‡ Associate Professor, Department of Anatomy and Neurobiology, and Division of Biology and Biomedical Sciences, † Research Assistant, Department of Anesthesiology, § Dr. Seymour and Rose T. Brown Professor, Department of Anesthesiology, Department of Developmental Biology, and Division of Biology and Biomedical Sciences, Washington University School of Medicine, St. Louis, Missouri.

Received from the Department of Anesthesiology, Washington University School of Medicine, St. Louis, Missouri. Submitted for publication May 11, 2011. Accepted for publication September 1, 2011. Supported by grants from the National Institute of Neurological Disorders and Stroke, Bethesda, Maryland (to Dr. Nonet; grant no. 5R01NS033535), and the National Institute of General Medical Sciences, Bethesda, Maryland (to Dr. Crowder; grant nos. 5R01GM059781 and 1R01GM055832).

Address correspondence to Dr. Crowder: Department of Anesthesiology, Washington University School of Medicine, 660 South Euclid Avenue, St. Louis, Missouri 63110. crowderm@morpheus.wustl.edu. Information on purchasing reprints may be found at [www.anesthesiology.org](http://www.anesthesiology.org) or on the masthead page at the beginning of this issue. ANESTHESIOLOGY's articles are made freely accessible to all readers, for personal use only, 6 months from the cover date of the issue.

Copyright © 2011, the American Society of Anesthesiologists, Inc. Lippincott Williams & Wilkins. Anesthesiology 2011; 115:1162–71

trations of isoflurane, which produces 0.62 mM aqueous concentration; isoflurane EC<sub>50</sub> against coordinated locomotion in *C. elegans* at 22°C = 0.7–1 vol%; 1 vol% isoflurane at 22°C = 0.58 mM).<sup>3–5</sup> Syntaxin is one of three essential presynaptic SNARE proteins that acts in concert with other proteins to mediate fusion of synaptic vesicles with the presynaptic membrane.<sup>6</sup> The unusual mutation, designated *unc-64(md130)*, produces a truncated syntaxin that dominantly antagonizes VA sensitivity along with expressing reduced wild-type syntaxin, resulting in other phenotypes consistent with decreased excitatory transmitter release. Importantly, other *unc-64* alleles with similarly decreased transmitter release phenotypes were hypersensitive to VAs; for example, *unc-64(md130)* has a 20–30-fold higher isoflurane EC<sub>50</sub> than the otherwise phenotypically similar VA hypersensitive *unc-64(md1259)* and *unc-64(js21)* mutants.<sup>5</sup> Thus, the truncated syntaxin is not indirectly antagonizing VA sensitivity by reducing transmitter release; rather, the data are most consistent with interaction of the truncated syntaxin with another protein essential for VA sensitivity.

To identify the relevant syntaxin-interacting protein(s) essential for VA sensitivity, we tested *C. elegans* mutants isolated in a screen for suppressors of syntaxin reduction-of-function phenotypes.<sup>7,8</sup> The logic of testing these mutants is that one or more of the suppressor mutations might lie in the putative syntaxin-interacting VA target and might be VA resistant. Indeed, we reported previously that some of these suppressors were VA resistant; however, the level of resistance was not as great as that in *unc-64(md130)* and was most likely attributable to an indirect effect on elevation of transmitter release.<sup>7</sup> Here we report on an additional syntaxin suppressor mutant whose level of resistance is similar to that of *md130* and define in part the mechanism whereby it regulates VA sensitivity in *C. elegans*.

## Materials and Methods

### C. elegans Strains and Transformants

Except where noted, *C. elegans* mutant strains were obtained from the *Caenorhabditis* Genetics Center, which is funded by the National Institutes of Health–National Center for Research Resources (Bethesda, Maryland). Strains were grown as described previously on nematode growth media agar.<sup>9</sup> N2 var Bristol was the wild-type strain and the genetic background for all mutants. Mutant strains used for this work are as follows: **LGI:** *unc-13(e376)*, *unc-13(e376)*; *acy-1(js127)III*, *unc-13(s69)*; *acy-1(js127)III*, *unc-13(s69)*, *gsa-1(ce81)*; **LGIII:** *unc-64(e246)*, *acy-1(js127)*, *acy-1(js127)/+*, *acy-1(js127) unc-64(e246)*, *acy-1(js127)/+ unc-64(e246)*, *acy-1(nu329)*, *acy-1(js127)*; *snb-1(md247)V*, *acy-1(js127)*; *unc-10(md1117)X*, *crh-1(n3315)*, *acy-1(js127)*, *crh-1(n3315)*, *unc-64(e246)*; *jsEx558[acy-1(P260S) Prol-6::GFP]*, *unc-64(e246)*; *jsEx570[acy-1(+)* Prol-6::GFP], *unc-64(e246)*; *jsEx571[acy-1(+)* Prol-6::GFP], *unc-64(e246)*; *jsEx575[acy-1(L2444S) Prol-6::GFP]*, *unc-64(e246)*; *jsEx579[Psnb-1::acy-1(P260S) Prol-6::GFP]*, *unc-*

*64(e246)*; *jsEx580[Pmyo-3::acy-1(P260S) Prol-6::GFP]*; **LGV:** *snb-1(md247)*; **LGX:** *unc-10(md1117)*, *kin-2(ce179)*; **Extra-chromosomal only:** *jsEx558[acy-1(P260S) Prol-6::GFP]*, *jsEx570[acy-1(+)* Prol-6::GFP], *jsEx571[acy-1(+)* Prol-6::GFP], *jsEx575[acy-1(L2444S) Prol-6::GFP]*, *jsEx579[Psnb-1::acy-1(P260S) Prol-6::GFP]*, *jsEx580[Pmyo-3::acy-1(P260S) Prol-6::GFP]*, *jsEx676[gsa-1(+)* Prol-6::GFP]. *js127* double mutants with *snb-1(md247)*, *unc-10(md1117)*, *unc-13(e376)*, and *unc-13(s69)* were constructed using *rbf-1(js232)*-marked Unc strains. *rbf-1* is located at the center of chromosome III and was used to mark the non-*js127* chromosome III. *js127;him-8* males were mated into *rbf-1;Unc* hermaphrodites and hyperactive (*js127* homozygous) progeny selected from the broods of heterozygous animals. The next generation was examined for nonhyperactive progeny (*js127;Unc*). Homozygosity of *md247* and *md1117* was verified molecularly, whereas *js127* was deduced by the absence of *js232* scored molecularly.

Germline transformation was accomplished by coinjecting the plasmid of interest, pBluescript carrier DNA (200 µg/ml), and the dominant transformation marker *rol-6::GFP* (pPHGFP1 at 20–35 µg/ml).<sup>10</sup> Transformants were selected by scoring green fluorescent protein (GFP) expression on an epifluorescence dissecting microscope, and stably transformed lines were isolated. *jsEx570* and *jsEx571* were obtained from injecting pPR1522 into *unc-64(e246)* at 15 µg/ml. A pAC2 (10 µg/ml) injection into *unc-64(e246)* yielded *jsEx558*, and a pAC3 (15 µg/ml) injection into *unc-64(e246)* produced *jsEx575*. pAC2 and pAC3 were also introduced independently into the balanced null allele *acy-1(pk1279)/dpy-17(e164)* to determine whether these altered forms were capable of rescuing null mutant lethality. pAC5 and pAC6 were each transformed into *unc-64(e246)* and the lines *jsEx579* and *jsEx580* isolated, respectively. Once stable lines were established, individual arrays were outcrossed to remove the *unc-64(e246)* mutation. *jsEx676* was created by the coinjection of pPD118.33 and pRP1505.

### Plasmid Constructs

pRP1522, a 14-kb genomic clone containing the *acy-1* locus,<sup>11</sup> was obtained from Celine Moorman, Ph.D. (Hubrecht Laboratory, Centre for Biomedical Genetics, Utrecht, The Netherlands) and Ronald Plasterk, Ph.D. (Professor, Hubrecht Laboratory, Centre for Biomedical Genetics). The single base pair *acy-1(js127)* lesion was introduced into this clone using the DpnI-mediated site-directed mutagenesis protocol<sup>12</sup> to create a genomic clone (pAC2) encoding the P260S mutant form of ACY-1. Specifically, pRP1522 was mutagenized using OL#897 (ATTCAGTCTGTGATGTCT-AAAAAGGTACGCA) and OL#898 (TGCGTACCTTTTGTAGACATCACAGACTGA AT). Similarly, pRP1522 was mutagenized using OL#955 (TTGGCAAGAAAGGATTCTGAGTTGGAGACACAG) and OL#956 (CTGTGTCTC-CAACTCAGAATCCTTTCTT GCCAA) to create pAC3, an *acy-1* genomic clone harboring an L244S lesion modeled after the constitutively active adenylate cyclase mutation isolated in *Dictyostelium*.<sup>13</sup> Both constructs

were sequenced to verify proper introduction of the desired lesion. Using this same mutagenesis method, a BamHI restriction site was engineered before the *acy-1* initiation site by mutagenizing pAC2 using OL#1026 (TCTT-GTCTTCTGGATCCATGGACGACGATGT) and OL#1027 (ACATCGTCGTCCTCA TGGATCCAGAAGACAAGA) to produce pAC4. The *acy-1* promoter was then replaced with the *snb-1* synaptobrevin promoter to yield a construct, pAC5, for selective expression of the P260S form in neurons. This was accomplished by swapping the SacII-BamHI fragment of pAC4 with the SacII-BamHI fragment of the polymerase chain reaction (PCR) product resulting from OL#1028 (GTTAGTATCATTC-GAAACATACC) and OL#1029 (AGCTTTCGCGGAAATC-TAGG) amplification of the *snb-1* promoter from pRM248. pAC6 was created in the same manner with OL#1028 and OL#1030 (GCTGCGGCCGCGGGTCGGC) used to amplify the *myo-3* promoter from pPD96.52 to study muscle selective expression. pPD118.33 is a *Pmyo-2::GFP*, and pRP1505 is a wild-type *gsa-1* construct and was obtained from Ronald Plasterk, Ph.D.<sup>14</sup>

### **unc-64(e246) Suppressor Screen**

A nonclonal genetic screen was performed using conventional mutagenesis.<sup>15</sup> *unc-64(e246)* L4-staged hermaphrodites were mutagenized for 4 h in 50 mM ethyl methanesulfonate. To recover recessive mutants, second generation self-progeny were examined for mobile animals. From a given plate of approximately 50–150 F1 progeny, at most one F2 candidate suppressor was selected and clonally passaged. Suppression was verified in the next generation, and subsequent backcrossing was initiated. This was generally performed by mating with wild-type males; F1 double heterozygous males were then crossed into *unc-64(e246)* and several Unc progeny hermaphrodites clonally passaged. The next generation was screened for moving animals to reticulate the *unc-64* Sup double mutants. After at least two rounds of backcrossing, suppressors were outcrossed from *unc-64(e246)* to obtain the single mutant suppressor. Presence of the suppressor was verified in the strain by reintroducing the *unc-64(e246)* allele and showing retention of suppression of paralysis. In seven rounds of screening a total of 24,000 haploid genomes, 14 suppressors were recovered. Other suppressors isolated in the screen have been described elsewhere.<sup>7,8</sup>

### **Genetic Mapping of Suppressors and Molecular Identification of Lesions**

All mapping and complementation tests were performed using standard genetic methods.<sup>16</sup> Suppressors were grouped initially based on their behavioral phenotype and subsequently placed into complementation groups by complementation assays. *js127* was a single allele isolate and was placed on chromosome III based on linkage to *lon-1*. Specifically, *js127 e246* males were mated into *lon-1 e246* hermaphrodites, resulting in *js127 e246/lon-1 e246* non-Lon cross progeny. These cross progeny were *e246* homozygous but were phenotypically non-Unc because of single copy

*js127* (i.e., *js127* acted dominantly to suppress the *e246* Unc phenotype). From this transheterozygote, 7 of 31 Lon progeny also were phenotypically non-Unc through acquisition of a single copy of *js127* by recombination. This localization was refined using three-factor mapping with *lon-1* and *dpy-18*. *lon-1 dpy-18 unc-64* was placed over *js127 e246*, and all 18 Lon non-Dpy recombinants failed to segregate *js127*, placing *js127* close by or to the left of *lon-1*. Fine structure mapping was performed using the single nucleotide polymorphisms of the Hawaiian strain, CB4856.<sup>17</sup> Single nucleotide polymorphisms that altered restriction enzyme recognition sites were chosen for analysis because they could be scored simply by PCR amplification of that genomic region and subsequent restriction enzyme digestion. First, a *dpy-1 daf-2 js127 lon-1 unc-64* strain was constructed by placing *dpy-1(e1) daf-2(e1370ts)* in trans to *js127 lon-1 unc-64*. 122 Sup Lon Unc progeny were passaged clonally, and nine plates contained Dpy Daf progeny. Dpy Daf animals were then raised at the permissive temperature, 20°C for *daf-2*, to assess locomotion to verify the presence of *js127*. Then, CB4856 males were mated into this strain, and the resulting cross progeny males were mated back into *dpy-1 daf-2 js127 lon-1 unc-64* hermaphrodites, to obtain at most one recombinant chromosome per progeny. Progeny of this cross were screened for Lon non-Daf animals, which would only result from a single recombination event between *daf-2* and *lon-1*. Two hundred thirty-nine recombinants were isolated, and then each recombinant chromosome was homozygosed and scored for *js127* by its Sup phenotype. The location of each recombination event was determined by scoring the genotype of each single nucleotide polymorphisms. PCR primers and location of single nucleotide polymorphisms are available upon request. Examination of the Sup Lon Unc class of recombinants placed *js127* to the right of cosmid F10F2, whereas information from the Lon Unc class of recombinants positioned *js127* to the left of cosmid C35D10. This region of approximately 273 Kb contained an estimated 82 genes, one of which was an adenylate cyclase gene, *acy-1*. Sequencing of the *acy-1* open reading frame from *js127* revealed a C > T single nucleotide change resulting in a P260S lesion in the protein. A PCR-digestion assay was developed to score the presence of this lesion molecularly. PCR amplification of a 210-bp product using OL#872 (TCTTGAA-GAGG-CCGATACATT) and OL#896 (AAAATGCAT-GCGTAGCCTTTTAG) followed by digestion with Bgl I resulted in a restriction pattern of 192 bp and 18 bp from wild type and a 210-bp undigested fragment from *js127*.

### **Behavioral and Drug Assays**

Locomotion assays were performed at room temperature (20–22°C) on at least 20 young adult hermaphrodites by collecting serial charge-coupled device camera images with an LG3 frame grabber (Scion Corporation, Frederick, MD) every 2.5–5 s at a magnification between 0.5× and 0.8×. Plates were undisturbed on the microscope for 5–10 min



before imaging was initiated. A series of images of basal locomotion were collected before dropping a metal rod from a constant height onto the plates to serve as a mechanical stimulus to excite the animals.<sup>18</sup> A similar series was collected after this mechanical stimulus. Locomotory velocity was calculated between successive images by measuring the linear displacement in the position of the tail of each animal. Velocities over four consecutive images were calculated and averaged to assess both basal and stimulated locomotion. Assays were performed in triplicate.

Acute sensitivity to the acetylcholinesterase inhibitor aldicarb was assayed by transferring 20–25 animals to plates containing aldicarb and monitoring the time course of animal paralysis.<sup>19</sup> Animals were counted as paralyzed if they appeared hypercontracted and failed to move even if prodded with a platinum wire. Aldicarb, 2-methyl-2-[methylthio]propionaldehyde O-[methylcarbamoyl]oxime, was obtained from Chem Services, Inc. (West Chester, PA) and prepared as a 100-mM stock solution in 70% ethanol. Aldicarb was added to the nutrient growth medium agar after autoclaving.

Isoflurane dispersal assays were performed at 22–24°C using young adult hermaphrodites, as described previously.<sup>20</sup> Worms were transferred in S-basal buffer to 9.5-cm agar dispersal plates seeded at their edge with *Escherichia coli* bacteria. Dispersal plates were then placed in various atmospheric concentrations of isoflurane (measured subsequently by gas chromatography) and the animals allowed to disperse. The fraction of adults (approximately 50 per assay plate) present in the bacterial ring divided by the total number of adults after 40 min was scored as the dispersal index.

### Cyclic Adenosine Monophosphate (cAMP) and Competitive Binding Assay

Endogenous cAMP concentrations were measured from young adult animals using a competitive binding enzyme-linked immunosorbent assay (Amersham Biosciences, Piscataway, NJ).<sup>21</sup> Wild-type, *acy-1(nu329)*, and *acy-1(js127)* animals were grown on the adenylate-cyclase-deficient *E. coli* strain DHP1F-glnV44(AS) recA1 endA1 gyrA96(NalR) thi1 hsdR17 spoT1 rfbD1 cyaA.<sup>22</sup> Synchronized cultures of adults were obtained using standard methods. Approximately 200  $\mu$ l packed adults were resuspended in 1 ml lysis buffer and sonicated with three 20-s pulses using a microtip. Protein concentrations were measured using a Bradford assay (Biorad, Hercules, CA). Assays were performed in triplicate.

### Statistical Analysis

Concentration/response curves were fit by nonlinear regression using the equation:  $y = \min + (\max - \min) / (1 + ([\text{Iso}] / \text{EC}_{50})^{-k})$ . The minimum was constrained to 0. The  $\text{EC}_{50}$ s were used as the measure of the isoflurane sensitivity of the strains.  $\text{EC}_{50}$ s were compared for statistical differences by simultaneous curve fitting, as described by Waud<sup>23</sup> using GraphPad Prism 5 Software (GraphPad, Software, Inc., San Diego, CA). The error values following the  $\text{EC}_{50}$  values are

the error of the fit. Error values for cAMP concentrations were SD of triplicate assays. Error values for aldicarb assays were SEM of triplicate assays. Locomotion rates and cAMP concentrations were compared by two-sided *t* test. The time at which half of the animals were paralyzed in the aldicarb paralysis assays was compared for statistical differences by simultaneous curve fitting using GraphPad Prism 5 Software. Statistically significant differences were at the  $P < 0.05$  level. For multiple comparisons, the significance threshold was less than 0.05 per number of comparisons.

## Results

The *js127* mutation was isolated in a screen for mutations that improve the locomotion of the *unc-64* syntaxin reduction-of-function allele, *e246*. *js127* strongly suppressed the slow uncoordinated locomotion of *unc-64(e246)* (fig. 1A, B). Indeed, after stimulation, the *js127 e246* double-mutant strain moved at speeds indistinguishable from wild-type animals and was the strongest suppressor mutant isolated in the screen (fig. 1B). To test whether this suppression of locomotion was associated with an increase in acetylcholine release, aldicarb sensitivities were measured. Aldicarb is an acetylcholinesterase inhibitor that is widely used to measure the levels of cholinergic transmission in *C. elegans* mutants with the caveat that aldicarb sensitivity is an indirect measure of transmitter release and only assays acetylcholine release.<sup>19</sup> Mutants with a decrease in acetylcholine release are more resistant to paralysis by aldicarb, and this can be conveniently measured by kinetic assays. *js127 e246* was significantly less resistant to aldicarb than was *unc-64(e246)* (fig. 1C), consistent with an enhancement of syntaxin's function to mediate synaptic vesicle fusion and transmitter release. The *js127* mutation was outcrossed from *unc-64(e246)*, and its isoflurane sensitivity was measured. *js127* was strongly resistant to isoflurane with an  $\text{EC}_{50}$  more than three times greater than that of the wild-type strain and fully resistant to concentrations of isoflurane in the clinical range (fig. 1D).

To identify the genetic lesion responsible for the phenotypes in *js127*, the suppression of the sluggish locomotion phenotype of *e246* was mapped genetically. The suppression phenotype mapped to a 273-Kb interval on the left arm of chromosome III (fig. 2A). The *C. elegans* genome sequence predicts 82 genes in this interval, one of which is *acy-1*, which encodes an adenylate cyclase previously shown to regulate neurotransmitter release in *C. elegans* and, by its closest homologs, in mammals.<sup>24–26</sup> The *acy-1* gene was sequenced in the *js127* mutant and a C > T transition mutation was found in codon 260, resulting in proline to serine missense lesion (fig. 2B). Proline 260 lies within a highly conserved region at the N-terminal end of the C1a domain, one of the cytoplasmic catalytic domains. To confirm that the P260S mutation was indeed responsible for the *js127* phenotypes, an *acy-1* genomic plasmid was constructed with the P260S mutation, and transgenic animals expressing the plasmid were generated. The P260S transgene strongly suppressed the locomotion

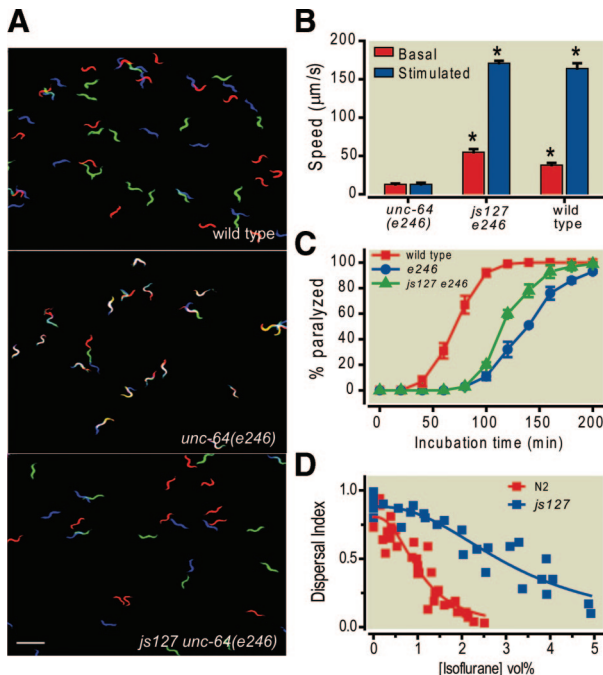


**Fig. 1.** Movement, transmitter release, and anesthetic phenotypes of the *js127* mutant. *js127* increases locomotion of *unc-64(e246)* mutants. Plates of the given genotype were tapped mechanically to stimulate locomotion; serial images were taken at various time points after stimulation and pseudocolored: red 0, green 30, and blue 60 s. Stationary animals that appear in the same location in all three serial images appear white. Scale bar = 1 mm (A). Measurements of locomotion speeds of *unc-64(e246)*, *js127 e246* and N2 wild-type animals. Speeds (mean  $\pm$  SE) before (basal) and after stimulation were calculated from serial images collected every 2.5–5 s from at least 20 animals moving on seeded agar plates (\*  $P < 0.0001$  vs. *unc-64(e246)*) (B). *js127* increases sensitivity of *unc-64(e246)* to aldicarb. Time course of paralysis of wild type, *unc-64(e246)*, and *js127 e246* on 1 mM aldicarb is shown. The increased rate of paralysis of *js127 e246* by aldicarb is significantly different from *e246* alone ( $P < 0.0001$ ) (C). Isoflurane resistance of *js127*. The dispersal index or fraction of adult worms that moves from the center of a 9.5-cm agar plate to the *E. coli*-seeded edge after a 40-min assay was measured during exposure to various concentrations of isoflurane. The  $EC_{50}$  for wild type is  $1.05 \pm 0.07$  and  $3.17 \pm 0.20$  for *js127*. *js127* is significantly more resistant to isoflurane than is N2 ( $P < 0.0001$ ) (D).

tion defects of *unc-64(e246)* to levels similar to those of the *js127e246* (fig. 2C). Likewise the transgene in the absence of *unc-64(e246)* conferred high-level isoflurane resistance, actually greater than that in *js127* [ $P < 0.007$  vs. *acy-1(js127)*] (fig. 2D). Based on the mapping, identification of a lesion, and phenocopy by transformation, we conclude that the C > T transition resulting in a P260S change in *acy-1* is the *js127* mutation. Confirming our assignment of *js127* to *acy-1*, this identical ACY-1(P260S) lesion was independently isolated in another laboratory in a similar screen for suppressors of a different mutation that reduces neurotransmitter release in

*C. elegans*.<sup>25</sup> This suggests that relatively few mutations in *acy-1* result in this phenotype.

The ability to reproduce the phenotypes of *js127* by transformation suggests that the mutation confers a gain of function to ACY-1. Consistent with this hypothesis, *js127* heterozygotes significantly suppress the sluggish locomotion of *unc-64(e246)* (fig. 3A). *js127* also dominantly confers an aldicarb hypersensitivity phenotype, whereas the reduction-of-function allele *acy-1(nu329)*<sup>27</sup> is aldicarb resistant (fig. 3B). Likewise for isoflurane sensitivity, the *acy-1(nu329)* allele has an isoflurane hypersensitive phenotype, opposite that of *acy-1(js127)* (fig. 3, C and D). However, unlike transgenic expression of ACY-1(P260S), transgenes expressing additional wild-type ACY-1 or ACY-1 with a mutation previously shown to confer constitutive activity on *Dictyostelium* adenylate cyclase<sup>13</sup> were not isoflurane resistant, nor did these transgenes suppress slow locomotion of *unc-64(e246)* phenotypes (fig. 3, D and E). Thus, P260S appears to be a particularly strong gain-of-function mutation. To test directly the hypothesis that *js127* was a gain-of-function mutation, we compared whole animal cAMP concentrations in *acy-1(js127)*, *acy-1(nu329)*, and wild-type animals. Consistent with the genetic data, cAMP concentrations were significantly higher in *js127* than in wild-type animals and significantly lower in *nu329* (fig. 3F). Thus, we conclude that *js127* confers an increase in ACY-1 adenylate cyclase activity.

ACY-1 is expressed throughout the *C. elegans* nervous system and in body wall muscles.<sup>14,27</sup> Thus, it is possible that enhanced ACY-1 activity in muscle cells, rather than neurons, is responsible for the *js127* phenotypes. To test this hypothesis, *acy-1(P260S)* was expressed selectively in neurons or muscle using cell-type-specific promoters. *acy-1(P260S)* driven by the pan-neuronal promoter *Psnb-1* strongly suppressed the slow locomotion of *unc-64(e246)*, whereas expression in muscle with the *Pmyo-3* promoter produced no discernible suppression (fig. 4A). Similarly, pan-neuronal *acy-1(P260S)* produced high-level resistance to isoflurane, whereas the isoflurane sensitivity of the muscle *acy-1(P260S)* was similar to that of wild type (fig. 4, B and C). We conclude that ACY-1 adenylate cyclase acts in neurons to suppress the syntaxin mutant phenotype and regulate isoflurane sensitivity.

To define the pathway whereby ACY-1 regulates transmitter release and isoflurane sensitivity, we tested the phenotypes of mutations in genes that might lie in the pathway. Adenylate cyclase normally is stimulated by G $\alpha$ s. *C. elegans* has one G $\alpha$ s gene, *gsa-1*, which has been shown to promote cholinergic transmitter release and neurodegeneration.<sup>14,24,25,27,28</sup> We found that similar to *acy-1(js127)*, an activating mutation, *ce81*,<sup>24</sup> in *gsa-1* was strongly resistant to isoflurane (fig. 5A). Likewise, animals transformed with additional copies of wild-type *gsa-1* were also isoflurane resistant (fig. 5A). Protein kinase A (PKA) is a classic downstream target of adenylate cyclases and has been implicated in ACY-1 signaling.<sup>25,29</sup>

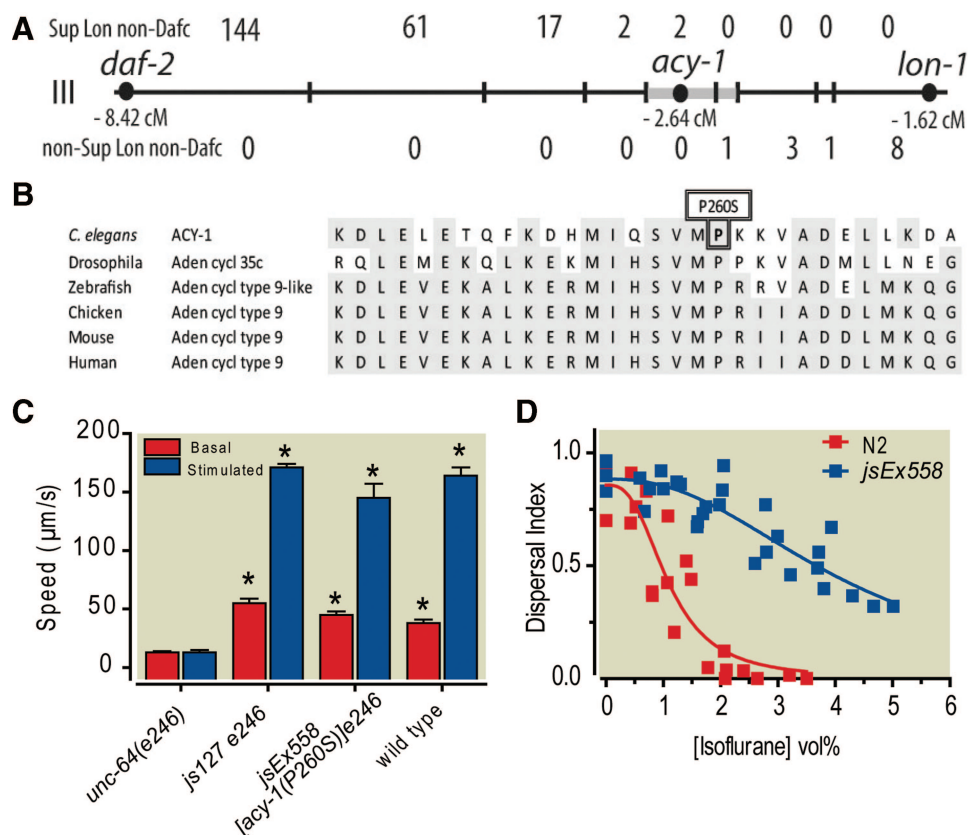


**Fig. 2.** *js127* is an allele of *acy-1*. *js127* mapping data. *js127* was mapped onto chromosome III between *daf-2* and *lon-1*. Two hundred thirty-nine recombinants between *daf-2* and *lon-1* were isolated after crossing into the highly sequence polymorphic CB4856 strain. The location and number of CB4856/N2 recombinants in classes that lie between consecutive pairs of single nucleotide polymorphisms are shown. The gray region indicates the smallest *js127* mapped interval (A). Alignment of the region around the *js127* mutation. The region surrounding the *js127* lesion was BLASTed against other organisms listed, and the highest hit was reciprocally BLASTed against ACY-1 to confirm best homology (B). Transformation phenocopy of *js127* suppression by an *acy-1* clone containing the P260S lesion into the e246 mutant phenocopies *js127* suppression of the e246 movement defect (C). *jsEx558[acy-1(P260S)]* transformant phenocopies the *js127* mutant for isoflurane resistance. The EC<sub>50</sub> for *jsEx558* is  $4.10 \pm 0.28$  and  $1.08 \pm 0.13$  for wild type. *jsEx558* is significantly more resistant to isoflurane than is N2 ( $P < 0.0001$ ) (D). Aden cycl = adenylate cyclase.

We tested a loss-of-function allele of *kin-2*, which encodes a negative regulatory subunit of PKA. Consistent with ACY-1 signaling through PKA to regulate isoflurane sensitivity, the *kin-2* loss-of-function mutant was strongly isoflurane resistant (fig. 5A). The cAMP response element binding protein (CREB) is a transcription factor that can be activated by PKA phosphorylation and regulates the expression of numerous genes.<sup>30</sup> CREB is most clearly implicated in synaptic plasticity and neural development but also has been shown to promote the expression of presynaptic syntaxin.<sup>31</sup> Thus, we considered the hypothesis that ACY-1 might promote synaptic transmission and reduce isoflurane sensitivity by activating CREB. However, a null mutation in the only *C. elegans* homolog of CREB,<sup>32</sup> *crh-1*, had normal sensitivity to isoflurane and did not suppress the isoflurane resistance of *js127* in the *acy-1(js127) crh-1*(null) double mutant (fig. 5A). The *crh-1*(null) mutant was resistant to aldicarb, consistent with the hypothesis that *crh-1* does promote cholinergic neurotransmission (fig. 5B); however, as for isoflurane resistance, the

*crh-1*(null) mutant did not suppress the aldicarb hypersensitivity phenotype of *acy-1(js127)*. A notable caveat to attributing the aldicarb-resistant phenotype to the *crh-1*(null) mutant is that only one mutant was tested and the phenotype was not rescued by transformation. Thus, the aldicarb resistance could be attributable to an unknown background mutation. However, the data definitively show that *C. elegans* CREB does not act downstream of ACY-1 to control neurotransmission and isoflurane sensitivity.

Finally, we tested for suppression of *js127* phenotypes by reduction of function mutations in three transmitter-release machinery proteins: UNC-10, rab-3-interacting molecule (RIM); SNB-1, synaptobrevin; and UNC-13, mUNC13. For isoflurane resistance and aldicarb sensitivity, the mutations in all three genes strongly suppressed *js127* (fig. 5, A and C, D, E). Thus, *js127* adenylate cyclase activation does not bypass the core vesicular fusion machinery to produce VA resistance or enhance transmitter release. However, for locomotion rate, only the locomotion of a strong *unc-13*



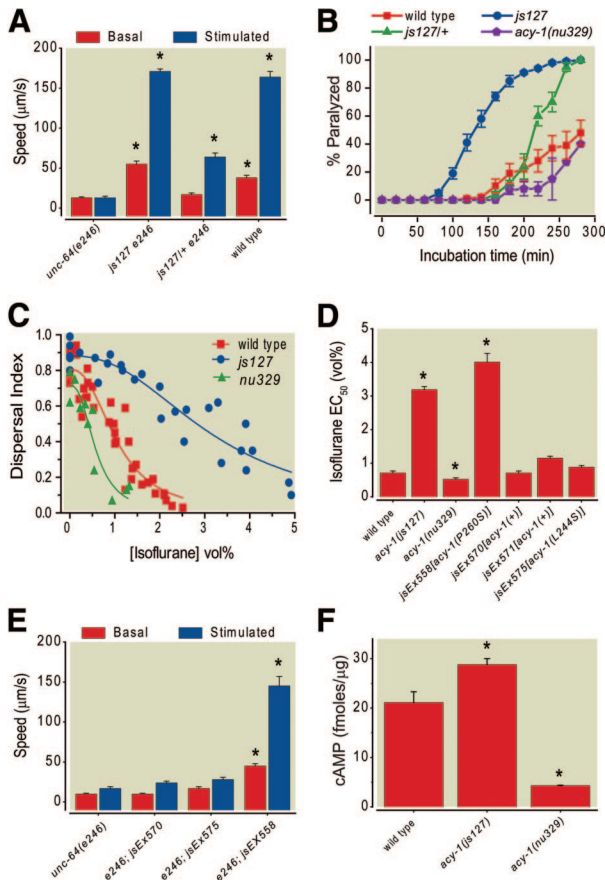


**Fig. 3.** *js127* is a gain of function *acy-1* allele. *js127* dominantly suppresses the locomotion defect of *e246*. *js127/+* indicates a heterozygous genotype (\*  $P < 0.01$  vs. corresponding *e246* value) (A). *js127* dominantly increases aldcarb sensitivity. *js127/+* is significantly hypersensitive to 0.35 mM aldcarb compared with wild type ( $P < 0.05$ ) (B). *acy-1(nu329 rf)* is a reduction of function allele of *acy-1<sup>27</sup>* and is hypersensitive to isoflurane. The  $\text{EC}_{50}$  for wild type is  $1.05 \pm 0.7$  compared with  $0.58 \pm 0.08$  for *nu329* ( $P < 0.002$ ) (C). *acy-1(+)* and L244S transformants do not confer isoflurane resistance. *jsEx570[acy-1(+)]* and *jsEx571[acy-1(+)]*, wild-type worms transformed with the *acy-1(+)* and *jsEx575[acy-1(L244S)]* had wild-type sensitivities to isoflurane (\*  $P < 0.01$  vs. wild type) (D). *acy-1(+)* and L244S transformants do not suppress the sluggish locomotion of *unc-64(e246)* (\*  $P < 0.01$  vs. *unc-64(e246)*) (E). Cyclic adenosine monophosphate (cAMP) levels increased in *js127*. Endogenous cAMP levels in wild type, *js127*, and *nu329* adult animals normalized to total protein (\*  $P < 0.05$  vs. wild type) (F).

allele (*s69*) was not improved by *js127* (fig. 5F). *unc-13(e376)*, a weaker allele, still moved significantly better in the background of *js127* (fig. 5F). Similarly, the locomotion rates of both *snb-1* partial loss of function and *unc-10* null mutants were improved significantly in a *js127* mutant background. Thus, UNC-10 and perhaps SNB-1 (the epistatic relationship of SNB-1 to ACY-1 is not definitive given the *snb-1* allele is not null) are not required for the locomotion-promoting activity of ACY-1. By contrast,

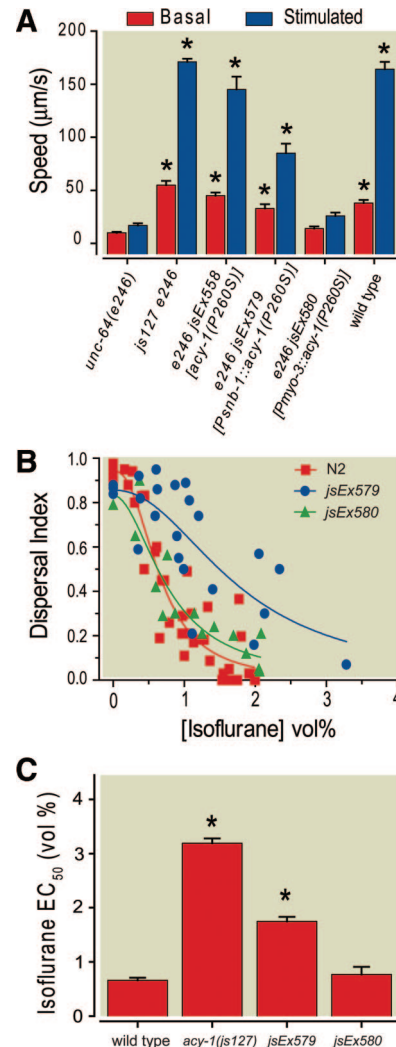


**Fig. 4.** *js127* functions in neurons. Locomotion speeds of *unc-64(e246)* transformed with various *acy-1* constructs. The locomotion defect of *e246* is significantly suppressed by the *js127* allele, *jsEx558[acy-1(P260S)]*, and *jsEx579[psnb-1::acy-1(P260S)]*, which is expressed only in neurons (\*  $P < 0.01$  vs. *e246*). *jsEx580[Pmyo-3::acy-1(P260S)]*, expressing only in muscle, does not suppress the *e246* movement defect (A). *jsEx579* is significantly resistant to isoflurane compared with wild type (B). Bar graph summary of information in B. (\*  $P < 0.0001$  vs. wild type) (C).

UNC-13, at least at the level of sensitivity of these assays, is epistatic to *acy-1(js127)*.

## Discussion

Through screening of mutations that suppress the phenotypes of a syntaxin reduction of function mutant, we have identified a gain-of-function mutation of *C. elegans* (ACY-1 adenylate cyclase) that strongly antagonizes isoflurane sensitivity. Our data are consistent with an ACY-1 signaling pathway as shown in figure 6. With regard to anesthetic mechanisms, the most central question posed by this study is whether ACY-1 is an anesthetic target and the *js127* muta-

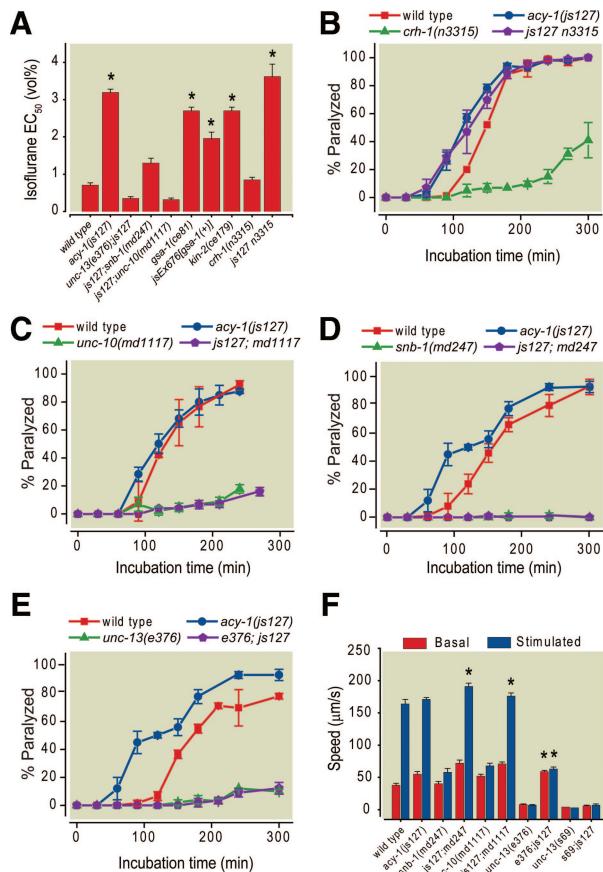


**Fig. 5.** Phenotypes of potential *acy-1* signaling pathway mutants. Isoflurane EC<sub>50</sub> values for various genes hypothesized to lie in the *acy-1* signaling pathway (\*  $P < 0.01$  vs. wild type) (A). *js127* increases sensitivity of *crh-1(n3315)* to 0.35 mM aldicarb ( $P < 0.01$ ) (B). Aldicarb resistance (0.35 mM) of *unc-10(md1117)* is not significantly suppressed by *js127* (C). Aldicarb resistance (0.35 mM) of *snb-1(md247)* is not significantly suppressed by *js127* (D). Aldicarb resistance (0.35 mM) of *unc-13(e376)* is not significantly suppressed by *js127* (E). *js127* mutation enhances the locomotion of several lethargic mutants but not *unc-13(s69)* (\*  $P < 0.01$  vs. lethargic single mutant) (F).

tion directly blocks volatile anesthetic inhibition of ACY-1. This hypothesis seems unlikely in light of our previous findings. Although not as VA resistant as *acy-1(js127)*, other mutants that suppress *unc-64(e246)* are also VA resistant.<sup>7</sup> In general, we have found that environmental conditions or mutations such as *acy-1(js127)* that enhance neurotransmitter release confer VA resistance.<sup>7,20,33</sup> Likewise, mutants with reduced neurotransmission have been found to be hypersensitive to VAs.<sup>5,20,33</sup> Thus, the anesthetic phenotype of *acy-1(js127)* is most easily explained as being attributable to indirect enhancement of the process that VAs block.

In *C. elegans*, only the truncated syntaxin and *unc-13* mutants have been found to deviate from the correlation between the levels of neurotransmitter release and VA resistance.<sup>5,34</sup> The truncated syntaxin acts in a dominant fashion to block VA effects on transmitter release without otherwise detectably altering

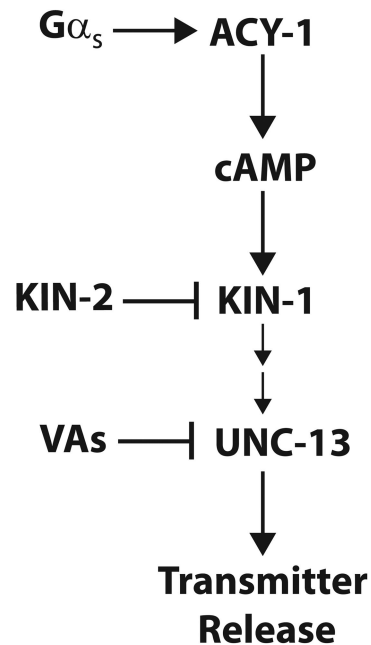


**Fig. 6.** Working model for ACY-1 signaling pathway regulating transmitter release and volatile anesthetic sensitivity. The model depicted is based on the genetic evidence and has not been confirmed by binding or electrophysiologic data. Volatile anesthetics (VAs) are shown inhibiting UNC-13, as previously proposed.<sup>34</sup> The direct target of the cyclic adenosine monophosphate (cAMP)-activated protein kinase A catalytic subunit KIN-1 is unknown but is unlikely to be UNC-13.

behavior or neurotransmission.<sup>5,34</sup> The VA resistance of the syntaxin mutant can be suppressed by overexpression of wild-type UNC-13, consistent with a model where the truncated syntaxin in a dose-dependent mechanism blocks VA inhibition of UNC-13 activity. The *unc-13* mutants, despite having reduced transmitter release, were also VA resistant, and a strain with a membrane-targeted UNC-13 was VA resistant, suggesting the model that VAs block membrane association of UNC-13.<sup>34</sup> Thus, we have previously proposed that UNC-13 is a presynaptic target for clinical concentration of VAs in *C. elegans*.<sup>34</sup>

Might UNC-13 be a direct target of PKA and thereby offer a testable hypothesis for the unusually strong VA resistance of *acy-1(js127)*? Indeed, among the release machinery mutants tested, only the strong *unc-13* allele, *s69*, was found to be incompetent for *js127* suppression of its uncoordinated locomotion. However, little spontaneous or evoked exocytosis is detected from cholinergic *unc-13(s69)* motor neurons by electrophysiologic assays.<sup>35–37</sup> Thus, although the formal interpretation of our genetic epistasis experiments is that UNC-13 lies downstream of ACY-1, this result may derive from the fact that *unc-13(s69)* has essentially no transmitter release for ACY-1 to enhance, rather than UNC-13 being the direct target of the GSA-1–ACY-1–PKA pathway. In addition, UNC-13-mUNC13 has not been reported to be a PKA target. It is more likely that PKA phosphorylates some intermediate target whose activity requires UNC-13. UNC-13 is



a diacyl glycerol-binding presynaptic protein that interacts with syntaxin, RIM, calmodulin, and other presynaptic proteins to promote neurotransmitter release.<sup>38</sup> A reasonable candidate PKA target is UNC-10 RIM. In mammals, PKA has been shown to phosphorylate RIM, and this phosphorylation is necessary for PKA-dependent presynaptic long-term potentiation in mouse cerebellar neurons.<sup>39–41</sup> RIM interaction with mUNC13 is necessary for normal synaptic vesicle priming in mouse hippocampal neurons,<sup>42</sup> and RIM binding to mUNC13 has been shown to reduce the concentrations of mUNC13 homodimers, which are autoinhibitory.<sup>43</sup> In addition to disinhibition of mUNC13, RIM has been shown to promote presynaptic localization of P- and Q-type calcium channels near the active zone and interact with other presynaptic proteins, including Rab3; it also may serve a scaffolding function.<sup>39,44,45</sup> However, in *C. elegans*, if UNC-10 RIM is the ACY-1/PKA target, it is not an essential target because *acy-1(js127)* is capable of significantly improving the locomotion of an *unc-10* null mutant. Likewise for the VA presynaptic mechanism, UNC-10 is non-essential because *unc-10* null mutants are normally sensitive to isoflurane.<sup>34</sup>

An alternative or additional ACY-1-PKA mechanism consistent with UNC-13 as the VA target is regulation of proteasome-dependent degradation of UNC-13. In *Drosophila* neurons, synaptic DUNC-13 (*Drosophila* UNC-13) concentrations were found to be positively regulated by cAMP and PKA.<sup>46</sup> Inhibition of cAMP-PKA signaling resulted in a rapid and substantial decrease in DUNC-13 concentrations at the synapse, and this decrease could be blocked with proteasome inhibitors. However, the mechanism whereby the cAMP-PKA pathway regulates the apparent proteasomal degradation of DUNC-13 is obscure.

Is the *C. elegans* presynaptic VA mechanism described here relevant to the mammalian anesthetic mechanism? As stated, presynaptic inhibition of excitatory neurotransmitter release has been demonstrated in a variety of mammalian models.<sup>1</sup> Thus, a contribution of presynaptic anesthetic effects to general anesthesia seems likely. The presynaptic machinery in *C. elegans* is highly conserved in humans,<sup>6,47</sup> and the VA concentrations to which the mutants in the presynaptic machinery are conferring resistance are in the clinical range. Thus, the *C. elegans* presynaptic VA mechanism further elaborated here might reasonably contribute to general anesthesia in mammals. Experimental support for this conjecture has been reported. A truncated syntaxin based on the *C. elegans* VA-resistant mutant was expressed in a rat neuroendocrine cell line and in hippocampus and found to antagonize the effects of clinical concentrations of isoflurane on neurosecretion and transmitter release.<sup>48</sup> These results argue that at least some aspects of the *C. elegans* presynaptic mechanism are conserved in higher organisms.

An important issue to consider when discussing the potential relevance of the proposed *C. elegans* presynaptic anesthetic mechanism to mammalian anesthesia is how to recon-

cile the fundamental function of UNC-13 orthologs with the differential inhibition by volatile anesthetics of transmitter release from distinct neuronal subtypes. In other words, if UNC-13 orthologs function at all synapses and are important presynaptic anesthetic targets, how might volatile anesthetics more potently inhibit excitatory synapses compared with inhibitory ones, as previously shown?<sup>1</sup> The mammalian UNC-13 homologs mUNC13-1, 2, and 3 have distinct functional roles that could contribute to the synapse-selective effects of VAs. Release from the majority of glutamatergic terminals in mouse hippocampus requires the mUNC13-1 isoform, whereas mUNC13-1 and mUNC13-2 function redundantly in  $\gamma$ -aminobutyric acid-mediated release, at least in the cerebral cortex and hippocampus.<sup>49</sup> In rat brain, mUNC13-1 is expressed throughout the central nervous system, whereas mUNC13-2 expression is restricted to the cerebral cortex and hippocampus. mUNC13-3 appears to be expressed exclusively in the cerebellum.<sup>50</sup> Intriguingly, mUNC13-1- and mUNC13-2-mediated release in mouse differs in their potentiation by diacyl glycerol; mUNC13-1 is less efficaciously potentiated.<sup>49</sup> These observations suggest the hypothesis that mUNC13-1, the closest homolog to *C. elegans* UNC-13, may be more sensitive to VAs because its weak DAG potentiation is more efficaciously blocked by VAs than is that of mUNC13-2. Testing of this hypothesis is experimentally feasible with the availability of mouse knockout strains for each of the mUNC13 isoforms.

## References

1. Hemmings HC Jr: Sodium channels and the synaptic mechanisms of inhaled anaesthetics. *Br J Anaesth* 2009; 103:61–9
2. Wu XS, Sun JY, Evers AS, Crowder M, Wu LG: Isoflurane inhibits transmitter release and the presynaptic action potential. *ANESTHESIOLOGY* 2004; 100:663–70
3. Crowder CM, Shebestor LD, Schedl T: Behavioral effects of volatile anesthetics in *Caenorhabditis elegans*. *ANESTHESIOLOGY* 1996; 85:901–12
4. Franks NP, Lieb WR: Selective actions of volatile general anaesthetics at molecular and cellular levels [published erratum appears in *Br J Anaesth* 1993;71:616]. *Br J Anaesth* 1993; 71:65–76
5. van Swinderen B, Saifee O, Shebestor L, Roberson R, Nonet ML, Crowder CM: A neomorphic syntaxin mutation blocks volatile-anesthetic action in *Caenorhabditis elegans*. *Proc Natl Acad Sci USA* 1999; 96:2479–84
6. Sudhof TC: The synaptic vesicle cycle. *Annu Rev Neurosci* 2004; 27:509–47
7. Hawasli AH, Saifee O, Liu C, Nonet ML, Crowder CM: Resistance to volatile anesthetics by mutations enhancing excitatory neurotransmitter release in *Caenorhabditis elegans*. *Genetics* 2004; 168:831–43
8. Wang ZW, Saifee O, Nonet ML, Salkoff L: SLO-1 potassium channels control quantal content of neurotransmitter release at the *C. elegans* neuromuscular junction. *Neuron* 2001; 32:867–81
9. Brenner S: The genetics of *Caenorhabditis elegans*. *Genetics* 1974; 77:71–94
10. Mello CC, Kramer JM, Stinchcomb D, Ambros V: Efficient gene transfer in *C. elegans*: Extrachromosomal maintenance and integration of transforming sequences. *EMBO J* 1991; 10:3959–70

11. Korswagen HC, van der Linden AM, Plasterk RH: G protein hyperactivation of the *Caenorhabditis elegans* adenylyl cyclase SGS-1 induces neuronal degeneration. *Embo J* 1998; 17:5059–65
12. Fisher CL, Pei GK: Modification of a PCR-based site-directed mutagenesis method. *Biotechniques* 1997; 23:570–1, 574
13. Parent CA, Devreotes PN: Constitutively active adenylyl cyclase mutant requires neither G proteins nor cytosolic regulators. *J Biol Chem* 1996; 271:18333–6
14. Korswagen HC, Park JH, Ohshima Y, Plasterk RH: An activating mutation in a *Caenorhabditis elegans* Gs protein induces neural degeneration. *Genes Dev* 1997; 11:1493–503
15. Anderson P: Mutagenesis, *Caenorhabditis elegans*: Modern Biological Analysis of an Organism. Edited by Epstein H, Shakes D. San Diego, Academic Press, 1995, pp 31–58
16. Herman RK, Horvitz HR: Genetic analysis of *Caenorhabditis elegans*, Nematodes as Biological Models. Edited by Zuckerman BM. New York, Academic Press, 1980; pp 227–61
17. Wicks SR, Yeh RT, Gish WR, Waterston RH, Plasterk RH: Rapid gene mapping in *Caenorhabditis elegans* using a high density polymorphism map. *Nat Genet* 2001; 28:160–4
18. Staunton J, Ganetzky B, Nonet ML: Rabphilin potentiates soluble *N*-ethylmaleimide sensitive factor attachment protein receptor function independently of rab3. *J Neurosci* 2001; 21:9255–64
19. Mahoney TR, Luo S, Nonet ML: Analysis of synaptic transmission in *Caenorhabditis elegans* using an aldicarb-sensitivity assay. *Nat Protoc* 2006; 1:1772–7
20. van Swinderen B, Metz LB, Shebestor LD, Crowder CM: A *Caenorhabditis elegans* pheromone antagonizes volatile anesthetic action through a go-coupled pathway. *Genetics* 2002; 161:109–19
21. Horton JK, Martin RC, Kalinka S, Cushing A, Kitcher JP, O'Sullivan MJ, Baxendale PM: Enzyme immunoassays for the estimation of adenosine 3',5' cyclic monophosphate and guanosine 3',5' cyclic monophosphate in biological fluids. *J Immunol Methods* 1992; 155:31–40
22. Hanahan D: Studies on transformation of *Escherichia coli* with plasmids. *J Mol Biol* 1983; 166:557–80
23. Waud DR: On biological assays involving quantal responses. *J Pharmacol Exp Ther* 1972; 183:577–607
24. Schade MA, Reynolds NK, Dollins CM, Miller KG: Mutations that rescue the paralysis of *Caenorhabditis elegans* ric-8 (synembryo) mutants activate the G alpha(s) pathway and define a third major branch of the synaptic signaling network. *Genetics* 2005; 169:631–49
25. Reynolds NK, Schade MA, Miller KG: Convergent, RIC-8-dependent Galpha signaling pathways in the *Caenorhabditis elegans* synaptic signaling network. *Genetics* 2005; 169:651–70
26. Seino S, Shibasaki T: PKA-dependent and PKA-independent pathways for cAMP-regulated exocytosis. *Physiol Rev* 2005; 85:1303–42
27. Berger AJ, Hart AC, Kaplan JM: G alphas-induced neurodegeneration in *Caenorhabditis elegans*. *J Neurosci* 1998; 18:2871–80
28. Jansen G, Thijssen KL, Werner P, van der Horst M, Hazendonk E, Plasterk RH: The complete family of genes encoding G proteins of *Caenorhabditis elegans*. *Nat Genet* 1999; 21:414–9
29. Hanoune J, Defer N: Regulation and role of adenylyl cyclase isoforms. *Annu Rev Pharmacol Toxicol* 2001; 41:145–74
30. Benito E, Barco A: CREB's control of intrinsic and synaptic plasticity: Implications for CREB-dependent memory models. *Trends Neurosci* 2010; 33:230–40
31. Sutton KG, McRory JE, Guthrie H, Murphy TH, Snutch TP: P/Q-type calcium channels mediate the activity-dependent feedback of syntaxin-1A. *Nature* 1999; 401:800–4
32. Bates EA, Victor M, Jones AK, Shi Y, Hart AC: Differential contributions of *Caenorhabditis elegans* histone deacetylases to huntingtin polyglutamine toxicity. *J Neurosci* 2006; 26:2830–8
33. van Swinderen B, Metz LB, Shebestor LD, Mendel JE, Sternberg PW, Crowder CM: Galpha regulates volatile anesthetic action in *Caenorhabditis elegans*. *Genetics* 2001; 158:643–55
34. Metz LB, Dasgupta N, Liu C, Hunt SJ, Crowder CM: An evolutionarily conserved presynaptic protein is required for isoflurane sensitivity in *Caenorhabditis elegans*. *ANESTHESIOLOGY* 2007; 107:971–82
35. Richmond JE, Davis WS, Jorgensen EM: UNC-13 is required for synaptic vesicle fusion in *C. elegans*. *Nat Neurosci* 1999; 2:959–64
36. Richmond JE, Weimer RM, Jorgensen EM: An open form of syntaxin bypasses the requirement for UNC-13 in vesicle priming. *Nature* 2001; 412:338–41
37. Madison JM, Nurrish S, Kaplan JM: UNC-13 interaction with syntaxin is required for synaptic transmission. *Curr Biol* 2005; 15:2236–42
38. Rizo J, Rosenmund C: Synaptic vesicle fusion. *Nat Struct Mol Biol* 2008; 15:665–74
39. Wang Y, Okamoto M, Schmitz F, Hofmann K, Südhof TC: Rim is a putative Rab3 effector in regulating synaptic-vesicle fusion. *Nature* 1997; 388:593–8
40. Castillo PE, Schoch S, Schmitz F, Südhof TC, Malenka RC: RIM1alpha is required for presynaptic long-term potentiation. *Nature* 2002; 415:327–30
41. Lonart G, Schoch S, Kaeser PS, Larkin CJ, Südhof TC, Linden DJ: Phosphorylation of RIM1alpha by PKA triggers presynaptic long-term potentiation at cerebellar parallel fiber synapses. *Cell* 2003; 115:49–60
42. Betz A, Thakur P, Junge HJ, Ashery U, Rhee JS, Scheuss V, Rosenmund C, Rettig J, Brose N: Functional interaction of the active zone proteins Munc13-1 and RIM1 in synaptic vesicle priming. *Neuron* 2001; 30:183–96
43. Deng L, Kaeser PS, Xu W, Südhof TC: RIM proteins activate vesicle priming by reversing autoinhibitory homodimerization of Munc13. *Neuron* 2011; 69:317–31
44. Pernia-Andrade A, Jonas P: The multiple faces of RIM. *Neuron* 2011; 69:185–7
45. Kaeser PS, Deng L, Wang Y, Dulubova I, Liu X, Rizo J, Südhof TC: RIM proteins tether  $Ca^{2+}$  channels to presynaptic active zones via a direct PDZ-domain interaction. *Cell* 2011; 144:282–95
46. Aravamudan B, Broadie K: Synaptic *Drosophila* UNC-13 is regulated by antagonistic G-protein pathways via a proteasome-dependent degradation mechanism. *J Neurobiol* 2003; 54:417–38
47. Richmond J: Synaptic function. *WormBook* 2005; 1–14
48. Herring BE, Xie Z, Marks J, Fox AP: Isoflurane inhibits the neurotransmitter release machinery. *J Neurophysiol* 2009; 102:1265–73
49. Rosenmund C, Sigler A, Augustin I, Reim K, Brose N, Rhee JS: Differential control of vesicle priming and short-term plasticity by Munc13 isoforms. *Neuron* 2002; 33:411–24
50. Augustin I, Betz A, Herrmann C, Jo T, Brose N: Differential expression of two novel Munc13 proteins in rat brain. *Biochem J* 1999; 337:363–71